

Phase-Based Image Matching and Its Application to Biometric Recognition

Koichi Ito* and Takafumi Aoki*

* Graduate School of Information Sciences, Tohoku University, Sendai, Japan.

E-mail: ito@aoki.ecei.tohoku.ac.jp Tel: +81-22-795-7169

Abstract—This paper presents an accurate image matching technique using phase information obtained by discrete Fourier transform of images and its application to biometric recognition. Most of biometric recognition algorithms employ computer vision, pattern recognition and image processing techniques or their combination. On the other hand, our approach using phase-based image matching is based on signal processing technique. Through a set of experiments for fingerprint, iris, face, palmprint and finger knuckle recognition, we demonstrate that our signal processing approach exhibits efficient performance for biometric recognition compared with the conventional approaches.

I. INTRODUCTION

Biometric authentication has been receiving extensive attention with the need for robust human recognition techniques in various networked applications [19]. Biometric authentication (or simply biometrics) is to identify a person based on the physiological or behavioral characteristics such as fingerprint, face, iris, voice, signature, etc. So far, a variety of biometric recognition algorithms which combines computer vision, pattern recognition and image processing techniques have been proposed. On the other hand, we have proposed a unified biometric recognition algorithm using the signal processing-based approach.

We consider employing the phase information obtained by Discrete Fourier Transform (DFT) of images. The phase information preserves the inherent features of the image, and its correlation function, called phase correlation or Phase-Only Correlation (POC), gives us both the good similarity measure for biometric recognition and the translational displacement for image registration. In particular, the image matching method using phase information called Band-Limited Phase-Only Correlation (BLPOC) has been proposed [18] and been successfully used in various biometric recognition algorithms [14], [27], [43]. BLPOC cannot handle the nonlinear deformation of images, since the phase information obtained from the entire image is employed. To deal with nonlinear deformation, the approach combined with phase-based correspondence matching [36] and BLPOC has been proposed [15], [7]. In this paper, we demonstrate the effectiveness of phase information for biometric recognition so as to prove that the signal processing technique is effective for biometric recognition problems.

II. PHASE-BASED IMAGE MATCHING

This section describes the fundamentals of phase-based image matching. We first introduce the importance of phase

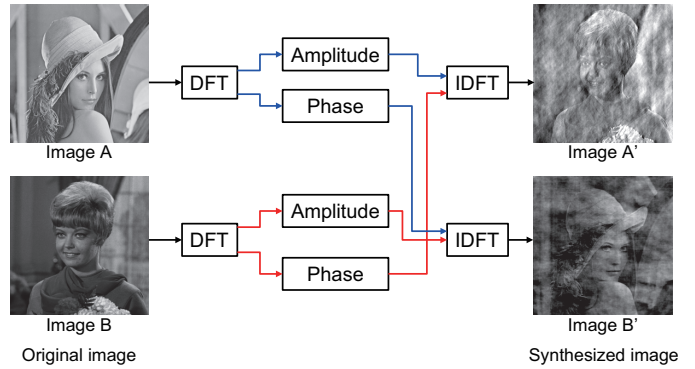


Fig. 1. The importance of phase information in images by replacing phase between images: Image A' with phase components of Image B looks like Image B. Similarly, Image B' with phase components of Image A looks like Image A. Therefore, the phase components contain the most important information to construct the image.

information in images, and describe the reason why we employ the phase features. Then, we describe Phase-Only Correlation (POC), Band-Limited POC (BLPOC), phase-based correspondence matching and local phase features.

A. The Importance of Phase Information in Images

The importance of the phase information in images has been reported in some literatures [24], [31]. In [31], Oppenheim said that many of the important features of a signal are preserved if only the phase is retained. We demonstrate the importance of phase information in images by replacing phase components between images as shown in Fig. 1 (Similar discussion has been given in Refs. [31], [34]). First, we calculate DFT of Image A and Image B, and obtain amplitude and phase components of each image. Next, we synthesize new frequency components of the image by replacing the phase components of Image A with those of Image B. Then, we calculate Inverse DFT (IDFT) of the synthesized frequency components and obtain the new images whose phase components are replaced. As observed in Fig. 1, the synthesized images are similar to the image having the corresponding phase components. This result indicates that the phase components contain the most important information to construct the image.

B. Phase-Only Correlation (POC)

As mentioned above, the phase components include the important information of the image. To use only the phase

components, we can perform accurate image matching. In this subsection, we introduce the principle of a POC function [24], [35].

Consider two $N_1 \times N_2$ images, $f(n_1, n_2)$ and $g(n_1, n_2)$, where we assume that the index ranges are $n_1 = -M_1, \dots, M_1$ ($M_1 > 0$) and $n_2 = -M_2, \dots, M_2$ ($M_2 > 0$) for mathematical simplicity, and hence $N_1 = 2M_1 + 1$ and $N_2 = 2M_2 + 1$. The discussion could be easily generalized to non-negative index ranges with power-of-two image size. Let $F(k_1, k_2)$ and $G(k_1, k_2)$ denote the 2D DFTs of $f(n_1, n_2)$ and $g(n_1, n_2)$, respectively. According to the definition of DFT [30], $F(k_1, k_2)$ and $G(k_1, k_2)$ are given by

$$\begin{aligned} F(k_1, k_2) &= \sum_{n_1, n_2} f(n_1, n_2) W_{N_1}^{k_1 n_1} W_{N_2}^{k_2 n_2} \\ &= A_F(k_1, k_2) e^{j\theta_F(k_1, k_2)}, \end{aligned} \quad (1)$$

$$\begin{aligned} G(k_1, k_2) &= \sum_{n_1, n_2} g(n_1, n_2) W_{N_1}^{k_1 n_1} W_{N_2}^{k_2 n_2} \\ &= A_G(k_1, k_2) e^{j\theta_G(k_1, k_2)}, \end{aligned} \quad (2)$$

respectively, where $k_1 = -M_1, \dots, M_1$, $k_2 = -M_2, \dots, M_2$, $W_{N_1} = e^{-j\frac{2\pi}{N_1}}$, $W_{N_2} = e^{-j\frac{2\pi}{N_2}}$, and \sum_{n_1, n_2} denotes $\sum_{n_1=-M_1}^{M_1} \sum_{n_2=-M_2}^{M_2}$. $A_F(k_1, k_2)$ and $A_G(k_1, k_2)$ are amplitude, and $\theta_F(k_1, k_2)$ and $\theta_G(k_1, k_2)$ are phase. The normalized cross power spectrum $R_{FG}(k_1, k_2)$ is given by

$$\begin{aligned} R_{FG}(k_1, k_2) &= \frac{F(k_1, k_2) \overline{G(k_1, k_2)}}{|F(k_1, k_2) \overline{G(k_1, k_2)}|} \\ &= e^{j\theta(k_1, k_2)}, \end{aligned} \quad (3)$$

where $\overline{G(k_1, k_2)}$ is the complex conjugate of $G(k_1, k_2)$ and $\theta(k_1, k_2)$ denotes the phase difference $\theta_F(k_1, k_2) - \theta_G(k_1, k_2)$. The POC function $r_{fg}(n_1, n_2)$ is the 2D Inverse DFT (2D IDFT) of $R_{FG}(k_1, k_2)$ and is given by

$$r_{fg}(n_1, n_2) = \frac{1}{N_1 N_2} \sum_{k_1, k_2} R_{FG}(k_1, k_2) W_{N_1}^{-k_1 n_1} W_{N_2}^{-k_2 n_2}, \quad (4)$$

where \sum_{k_1, k_2} denotes $\sum_{k_1=-M_1}^{M_1} \sum_{k_2=-M_2}^{M_2}$. When two images are similar, their POC function gives a distinct sharp peak. When two images are not similar, the peak drops significantly. The height of the peak gives a good similarity measure for image matching, and the location of the peak shows the translational displacement between the images.

We have proposed a high-accuracy translational displacement estimation method, which employs (i) an analytical function fitting technique to estimate the sub-pixel position of the correlation peak, (ii) a windowing technique to eliminate the effect of periodicity in 2D DFT, and (iii) a spectrum weighting technique to reduce the effect of aliasing and noise [35].

C. Band-Limited POC (BLPOC)

We have proposed a BLPOC function [18] dedicated to biometric recognition tasks. The idea to improve the matching

performance is to eliminate meaningless high frequency components in the calculation of normalized cross power spectrum R_{FG} depending on the inherent frequency components of images. Assume that the ranges of the inherent frequency band are given by $k_1 = -K_1, \dots, K_1$ and $k_2 = -K_2, \dots, K_2$, where $0 \leq K_1 \leq M_1$ and $0 \leq K_2 \leq M_2$. Thus, the effective size of frequency spectrum is given by $L_1 = 2K_1 + 1$ and $L_2 = 2K_2 + 1$. The BLPOC function is given by

$$r_{fg}^{K_1 K_2}(n_1, n_2) = \frac{1}{L_1 L_2} \sum'_{k_1, k_2} R_{FG}(k_1, k_2) W_{L_1}^{-k_1 n_1} W_{L_2}^{-k_2 n_2}, \quad (5)$$

where $n_1 = -K_1, \dots, K_1$, $n_2 = -K_2, \dots, K_2$, and \sum'_{k_1, k_2} denotes $\sum_{k_1=-K_1}^{K_1} \sum_{k_2=-K_2}^{K_2}$. Note that the maximum value of the correlation peak of the BLPOC function is always normalized to 1 and does not depend on L_1 and L_2 .

D. Phase-based correspondence matching

In order to handle the nonlinear deformation of images, we employ the sub-pixel correspondence matching using POC [36], which employs (i) a coarse-to-fine strategy using image pyramids for robust correspondence search and (ii) a sub-pixel translational displacement estimation method using POC for local block matching. Let p be a coordinate vector of a reference pixel in the reference image $I(n_1, n_2)$. The problem of sub-pixel correspondence search is to find a real-number coordinate vector q in the input image $J(n_1, n_2)$ that corresponds to the reference pixel p in $I(n_1, n_2)$. We briefly explain the procedure as follows.

Step 1: For $l = 1, 2, \dots, l_{\max}$, create the l -th layer images $I_l(n_1, n_2)$ and $J_l(n_1, n_2)$, i.e., coarser versions of $I_0(n_1, n_2)$ ($= I(n_1, n_2)$) and $J_0(n_1, n_2)$ ($= J(n_1, n_2)$), recursively as follows:

$$I_l(n_1, n_2) = \frac{1}{4} \sum_{i_1=0}^1 \sum_{i_2=0}^1 I_{l-1}(2n_1 + i_1, 2n_2 + i_2), \quad (6)$$

$$J_l(n_1, n_2) = \frac{1}{4} \sum_{i_1=0}^1 \sum_{i_2=0}^1 J_{l-1}(2n_1 + i_1, 2n_2 + i_2). \quad (7)$$

Step 2: Estimate the displacement between $I_{l_{\max}}(n_1, n_2)$ and $J_{l_{\max}}(n_1, n_2)$ with pixel accuracy using POC-based image matching. Let the estimated displacement vector be $\delta_{l_{\max}}$.

Step 3: For every layer $l = 1, 2, \dots, l_{\max}$, calculate the coordinate $p_l = (p_{l,1}, p_{l,2})$ corresponding to the original reference point p_0 ($= p$) recursively as follows:

$$p_l = \left\lfloor \frac{1}{2} p_{l-1} \right\rfloor = \left(\left\lfloor \frac{1}{2} p_{l-1,1} \right\rfloor, \left\lfloor \frac{1}{2} p_{l-1,2} \right\rfloor \right), \quad (8)$$

where $\lfloor z \rfloor$ denotes the operation to round the element of z to the nearest integer towards minus infinity.

Step 4: We assume that $q_{l_{\max}} = p_{l_{\max}} + \delta_{l_{\max}}$ in the coarsest layer. Let $l = l_{\max} - 1$.

Step 5: From the l -th layer images $I_l(n_1, n_2)$ and $J_l(n_1, n_2)$, extract two sub-images (or image blocks) $f_l(n_1, n_2)$ and

$g_l(n_1, n_2)$ with their centers on p_l and $2q_{l+1}$, respectively. The size of image blocks is $W_c \times W_c$ pixels.

Step 6: Estimate the displacement between $f_l(n_1, n_2)$ and $g_l(n_1, n_2)$ with pixel accuracy using POC-based image matching. Let the estimated displacement vector be δ_l . The l -th layer correspondence q_l is determined as follows:

$$q_l = 2q_{l+1} + \delta_l. \quad (9)$$

Step 7: Decrement the counter by 1 as $l \leftarrow l - 1$ and repeat from Step 5 to Step 7 while $l \geq 0$.

Step 8: From the original images $I_0(n_1, n_2)$ and $J_0(n_1, n_2)$, extract two image blocks with their centers on p_0 and q_0 , respectively. Estimate the displacement between the two blocks with sub-pixel accuracy using POC-based image matching. Let the estimated displacement vector with sub-pixel accuracy be denoted by $\delta = (\delta_1, \delta_2)$. Update the corresponding point as follows:

$$q = q_0 + \delta. \quad (10)$$

The peak value of the POC function is also obtained as a measure of reliability in local block matching.

E. Local Phase Features

We have proposed local phase features extracted from each layer of multi-scale image pyramids, which are designed specifically for biometric recognition [8]. Using the proposed local phase features, we can align the global translation between images in the top (or coarsest) layer, align the minute translation between local block images in the middle layer, and finally evaluate the similarity between local block images in the bottom (or original image) layer. The amount of local phase features can also be reduced by phase quantization without sacrificing the performance of biometric recognition.

III. APPLICATION TO BIOMETRIC RECOGNITION

In this section, we show application of phase-based image matching to biometric recognition such as fingerprint, iris, face, palmprint, finger knuckle and multibiometric recognition.

A. Fingerprint Recognition

Among all the biometric traits, a fingerprint is the most popular biometric trait and is successfully used in many person authentication applications [25]. Major approaches for fingerprint recognition today can be broadly classified into feature-based approach [20], [21] and correlation-based approach [38], [18]. Typical fingerprint recognition methods employ feature-based matching, where minutiae (i.e., ridge ending and ridge bifurcation) are extracted from the registered fingerprint image and the input fingerprint image, and the number of corresponding minutia pairs between the two images is used to recognize a valid fingerprint image [25]. The feature-based matching is highly robust against nonlinear fingerprint distortion, but shows only limited capability for recognizing poor-quality fingerprint images with low S/N due to unexpected fingertip conditions (e.g., dry fingertips, rough fingertips, allergic-skin fingertips) as well as weak impression of fingerprints. On the other hand, as one of the efficient



Fig. 2. Examples of genuine pairs from FVC2002 DB1, which are difficult to verify due to (a) nonlinear distortion and (b) small overlap.

TABLE I
EERs FOR INDIVIDUAL FINGERPRINT MATCHING ALGORITHMS.

Algorithm	FVC2002 DB1
A	3.06%
B	5.57%
C	2.89%
D	5.27%

correlation-based approaches is to employ POC [18]. The use of Fourier phase information of fingerprint images makes it possible highly reliable fingerprint matching for low-quality fingerprints whose minutiae are difficult to be extracted as mentioned above. However, the performance of the POC-based fingerprint matching is degraded by nonlinear distortion in fingerprint images.

Each approach employs different matching criteria to compute a matching score which is used for authentication, since the minutiae-based matching uses local information of a fingerprint while the correlation-based matching uses global information of a fingerprint [17]. We have developed the three different types of feature-based fingerprint matching algorithm: (i) structure matching [21], (ii) string matching [20] and (iii) block matching [16], which are combined with phase-based image matching to improve the matching performance of fingerprint matching. To combine fingerprint matching algorithms, we employ a score-level fusion method which is one of the most convenient method for combination of matchers [33].

In the experiment, we use FVC2002 set A [2] for evaluating fingerprint matching performance. A set of fingerprint images in this database is captured with an optical sensor (Touch View II, Identix Incorporated, 500dpi) of size 388×374 pixels, which contains 800 fingerprint images from 100 different subjects with 8 impressions for each finger. Figure 2 shows two examples of genuine pairs, which are difficult to verify due to nonlinear distortion and small overlap. We first evaluate genuine matching scores for all the possible combinations of genuine attempts; the number of attempts is ${}_8C_2 \times 100 = 2,800$. Next, we evaluate imposter matching scores for imposter attempts: the number of attempts is ${}_{100}C_2 = 4,950$, where we select a single image (the first image) for each fingerprint and make all the possible combinations of imposter attempts.

We compare four fingerprint matching algorithms: (A) POC-based matching, (B) structure matching, (C) string matching and (D) block matching. The performance of the biometrics-

TABLE II
THE BEST COMBINATION OF FINGERPRINT MATCHING ALGORITHMS AND ITS EER.

Combination	EER [%]	Weight
A, B×C, D	0.61	(0.30, 0.55, 0.15)

based verification system is evaluated by the Receiver Operating Characteristic (ROC) curve, which illustrates the False Reject Rate (FRR) against the False Accept Rate (FAR) at different thresholds on the matching score. The Equal Error Rate (EER) is also used to summarize performance of a verification system. The EER is defined as the error rate where $1FRR = FAR$. Table I summarizes EERs for each algorithm. The matching performance of the feature-based algorithms (B)–(D) is comparable with the POC-based algorithm (A).

We evaluate the matching performance of the combined algorithm. In this experiment, we employ the weighted sum rule to combine matching scores from the algorithms (A)~(D). In order to determine the optimal values of weights, we evaluate EERs for all the combinations by changing the weight for each matching score from 0.00 to 1.00 at intervals of 0.05, where the sum of weights is always 1. Hence, the total number of weight patterns which we consider in this optimization process is 4,473 patterns for all the matching score combinations. Table II shows the best combination of the algorithms (A)~(D). The EER is 0.61% when using the weighted sum rule, where the weight is 0.30 for (A), 0.55 for (B)×(D) and 0.15 for (C). Our observation indicates that the combination of the correlation-based matching and the feature-based matching is effective for improving matching performance, since these algorithms play a complementary role for fingerprint matching tasks.

B. Iris Recognition

The human iris, which is the annular part between the pupil and the white sclera, has a complex pattern determined by the chaotic morphogenetic processes during embryonic development. The iris pattern is unique to each person and to each eye and is essentially stable over a lifetime. A famous iris recognition algorithm is iriscode which was proposed by Daugman [10]. 2D Gabor filters are used to extract a feature vector corresponding to a given iris image. Then, the filter outputs are quantized to generate a 2-Kbit iriscode. The dissimilarity between a pair of iriscodes is measured by their Hamming distance. The iriscode is very compact and accurate, while the matching performance is significantly influenced by many parameters in the feature extraction process.

Addressing the problem, we have proposed an iris recognition algorithm using BLPOC [27] whose matching process is similar to the fingerprint recognition algorithm using BLPOC [18]. The proposed algorithm consists of 4 steps: (i) preprocessing, (ii) effective region extraction, (iii) displacement alignment and (iv) matching score calculation. In the preprocessing (i), we localize the iris region in the captured image and produce a normalized iris texture image with a fixed

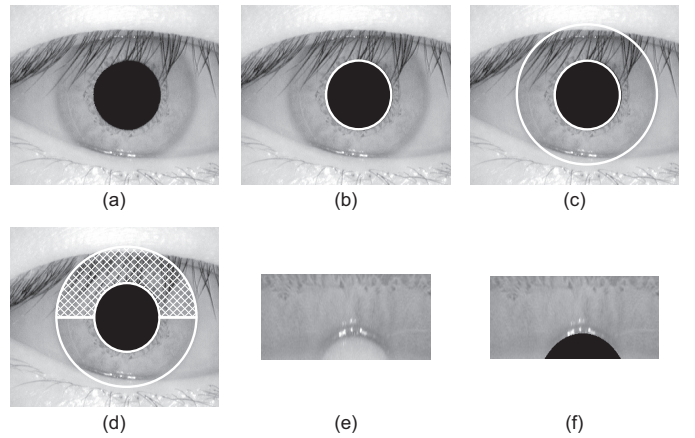


Fig. 3. Preprocessing for iris recognition: (a) iris image, (b) detected inner boundary, (c) detected outer boundary, (d) lower half of the iris region for matching, (e) normalized image and (f) normalized image with eyelid masking.

size as shown in Fig. 3. In the effective region extraction (ii), we extract the effective regions of the same size from two images. In the displacement alignment (iii), we align the translational displacement between extracted images to normalize the rotation of the camera, head tilt and rotation of the eye. In the matching score calculation (iv), we calculate the BLPOC function between the aligned images and evaluate the highest correlation peak value as a matching score. For degraded iris images, we can modify the above algorithm by introducing a spatial ensemble averaging of the BLPOC function [27].

To evaluate the performance of iris recognition algorithms, we use two databases: CASIA iris image database (ver. 1.0 and 2.0) [1] and ICE 2005 database [3]. CASIA iris image database ver. 1.0 contains 756 gray-scale eye images (320×280 pixels) with 108 eyes and 7 different images of each eye. In the experiment, we evaluate the genuine matching scores for 2,268 pairs and the imposter matching scores for 283,122 pairs. To compare the performance of the proposed algorithm with iriscode, we use the iris recognition algorithm using 1D log-Gabor filter [26]. The EER of the proposed algorithm is 0.0032%, while the algorithm using 1D log-Gabor filter is 1.46%. CASIA iris image database ver. 2.0 contains 1,200 gray-scale eye images (640×480 pixels) with 60 eyes and 20 different images of each eye. We evaluate the genuine matching scores for 11,400 pairs and the imposter matching scores for 28,320 pairs. The EER of the proposed algorithm is 0.53%. ICE 2005 database contains 2,953 gray-scale images (640×480 pixels) from 124 right eyes and 120 left eyes (1,425 images are from the right eyes and 1,528 images are from the left eyes). NIST prepares two experiments: Experiment 1 includes 12,214 genuine pairs and 1,002,386 pairs and Experiment 2 includes 14,653 genuine pairs and 1,151,975 imposter pairs. The EER for Experiment 1 is 0.33%, while that for Experiment 2 is 1.21%. As observed in the above experimental results, the proposed algorithm exhibits efficient

performance for iris recognition problems.

C. Face Recognition

The phase-based image matching technique is also effective for face recognition problems [13]. Unlike fingerprint and iris recognition problems, face images may have nonlinear deformation due to head pose change, occlusions, expression changes, etc. Therefore, we cannot apply the same approach of fingerprint and iris recognition problems to the face recognition problem. Addressing this problem, we employ the fact that the nonlinear deformation can be approximated by minute translations. Hence, we can use the phase-based correspondence matching approach to achieve accurate face recognition.

The proposed algorithm consists of 4 steps: (i) normalization, (ii) reference point placement, (iii) correspondence matching and (iv) matching score calculation. In the normalization (i), we normalize scale, rotation and illumination of face images. In this paper, we employ the normalization tool in the CSU Face Identification Evaluation System [9]. In the reference point placement (ii), we place a set of reference points of the normalized face image for correspondence matching. In the correspondence matching (iii), we find the corresponding points on the input image from the reference points on the registered image. In the matching score calculation (iv), we calculate the matching score between the images according to the number of correct corresponding points, where the correct corresponding point means that the correlation peak value is over the threshold.

The performance of the proposed algorithm is evaluated by using the CSU Face Identification Evaluation System [9] with the FERET database [32]. The CSU Face Identification Evaluation System includes conventional face recognition algorithms for comparison. The conventional algorithms compared in the experiments are Bayesian algorithm [28], EBGM algorithm [39], LDA-based algorithm [47] and PCA-based algorithm [37]. We also employ LBP-based face recognition algorithms [6] to demonstrate effectiveness of the proposed algorithm. The FERET database contains 3,368 face images of 1,209 subjects. The face images in the FERET database are organized into a gallery set (*fa*) and 4 probe sets such as *fb*, *fc*, *dup1* and *dup2*. The images in *fa* and *fb* set were taken in the same session with the same camera and illumination condition, but with different expression. The images in *fc* set were taken in the same session using the different camera and lighting. The images in *dup1* set were taken later in time. The images in *dup2* set which is a subset of *dup1* set were taken at least a year. Using the FERET database, we perform 4 experiments denoted by *fafb*, *fafc*, *dup1* and *dup2*.

Table III shows the recognition rates of genuine pairs at rank 1 for each experiment. As for experiments *fafb* and *fafc*, the recognition rate for the proposed algorithms is more than 99% at rank 1. This result indicates that the proposed algorithm are robust against facial expression changes and illumination changes. As for experiments *dup1* and *dup2*, the recognition rate of the proposed algorithm is more than 88% at rank 1. The performance of the proposed algorithm is slightly dropped

TABLE III
RECOGNITION RATE FOR THE PROPOSED ALGORITHM AND COMPARISON ALGORITHMS USING THE FERET DATABASE.

Algorithm	<i>fafb</i>	<i>fafc</i>	<i>dup1</i>	<i>dup2</i>
Bayesian	82.1%	38.1%	53.0%	32.1%
EBGM	93.5%	78.4%	57.3%	46.6%
LDA	71.6%	44.3%	44.0%	16.2%
PCA	85.3%	65.5%	44.3%	21.8%
LBP	97.0%	79.0%	66.0%	64.0%
Proposed	99.7%	100.0%	88.8%	88.9%

due to face images having expression changes, illumination changes, aging, etc. Nevertheless, the recognition rate of the proposed algorithm is still higher than the conventional algorithms. As a result, the proposed algorithm is robust against illumination change, facial expression change and aging compared with the conventional algorithms.

D. Palmprint Recognition

A palmprint, the large inner surface of a hand, contains many features such as principle lines, ridges, minutia points, singular points and texture, and is expected to be more distinctive than a fingerprint [40], [23]. Conventional algorithms for palmprint recognition extract feature vectors corresponding to individual palmprint images and perform palmprint matching based on some distance metrics [11], [41], [22]. Another algorithm employs correlation filters to classify and recognize palmprint images [12]. On the other hand, we have proposed a palmprint recognition algorithm using POC [14]. The recognition performance of these algorithms is degraded for palmprint images having nonlinear distortion due to movement of a hand and fingers, since these algorithms consider only the rigid body transformation between palmprint images. To address the above problem, we can use the phase-based correspondence matching approach [15] as well as face recognition.

The proposed algorithm consists of 2 steps: (i) preprocessing and (ii) matching. In the preprocessing (i), we extract a palmprint region, which is the center part of a palm, from the input image. We employ the method described in [41]. This method uses gaps between fingers as reference points to define the palmprint region as shown in Fig. 4. In the matching (ii), we evaluate the matching score between the palmprint regions according to the number of corresponding points obtained by the phase-based correspondence matching between the regions.

The performance of the proposed algorithm is evaluated using the PolyU Palmprint Database [5]. This database consists of 600 images (384×284 pixels) with 100 subjects and 6 different images of each palmprint. We evaluate the genuine matching scores for 1,500 pairs and the imposter matching scores for 178,200 pairs. We compare the performance of the proposed algorithm with the two conventional algorithms: Zhang [41] and Ito [14]. The EER of the proposed algorithm is 0.003%, while that of Zhang is 2.147% and that of Ito is 0.200%. As is observed in the above experiments, the proposed algorithm is particularly useful for verifying palmprint images.

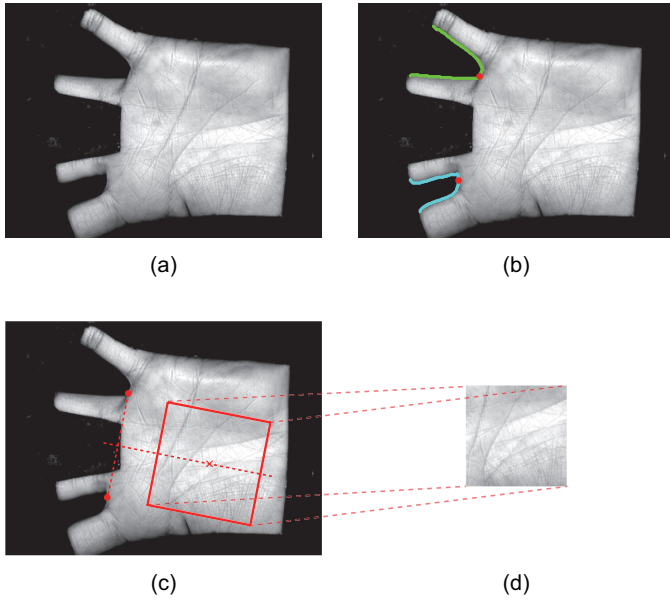


Fig. 4. Example of palmprint region extraction: (a) palmprint image, (b) gaps between index and middle fingers and between ring and little fingers, (c) palmprint region in the palmprint image and (d) extracted palmprint region.

E. Finger Knuckle Recognition

A finger knuckle pattern is a pattern of outer finger knuckle surface which contains many fine ridge patterns and texture, and is expected to be one of the distinctive biometric traits. The recognition performance of the finger knuckle recognition algorithms may be degraded for the images having nonlinear deformation due to the movement of a finger. To achieve accurate finger knuckle recognition, we consider such nonlinear deformation during finger knuckle matching.

We have proposed a finger knuckle recognition algorithm using BLPOC-based local block matching [7]. First, we correct the global transformation between finger knuckle images which is estimated using phase-based correspondence matching. Next, we correct the minute translational displacement between each local image block pair using the BLPOC-based local block matching. Finally, we take the average of a set of the BLPOC functions calculated from each local image block pair and obtain the correlation peak value of the average BLPOC function as a matching score between the finger knuckle images.

We evaluate the performance of finger knuckle recognition algorithms using the PolyU FKP database [4]. The PolyU FKP database consists of 7,920 images (384×288 pixels) with 165 subjects and 6 different images for each of the left index finger, the left middle finger, the right index finger and the right middle finger in 2 separate sessions. In the experiment, the images in the first session belong to the gallery set, while the images in the second session belong to the probe set, where each session consists of 660 (165×4) classes and 3,960 (660×6) images. In the PolyU FKP database, ROI images extracted by the method proposed in Ref. [45] are also included, where

TABLE IV
EERS AND d' OF THE FKP RECOGNITION ALGORITHMS.

Algorithm	EER [%]	d'
OE-SIFT [29]	0.850	—
CompCode [46]	1.658	4.2989
ImCompCode & MagCode [46]	1.475	4.3224
BLPOC [46]	1.676	2.4745
LGIC [46]	0.402	4.5356
LGIC ₂ [44]	0.358	4.7001
Proposed	0.321	6.9424

the image size of ROI is 220×110 pixels. We evaluate the genuine matching scores for 23,760 pairs and the imposter matching scores for 15,657,840 pairs.

Table IV shows the EERs [%] and d' values of finger knuckle recognition algorithms: OE-SIFT [29], CompCode [42], ImCompCode & MagCode [45], BLPOC [43], LGIC [46], LGIC₂ [44] and the proposed algorithm. d' is the index of how well the genuine and the imposter distributions are separated and is given by

$$d' = \frac{\sqrt{2} |\mu_{\text{genuine}} - \mu_{\text{impostor}}|}{\sqrt{\sigma_{\text{genuine}}^2 + \sigma_{\text{impostor}}^2}}, \quad (11)$$

where μ_{genuine} and μ_{impostor} are the mean value of genuine and imposter matching scores, respectively, and σ_{genuine} and σ_{impostor} are the standard deviation of genuine and imposter matching scores, respectively. Note that EERs and d' for the conventional algorithms are referred from cited papers in Table IV, where the experimental conditions such as the number of genuine and imposter pairs are the same in all the algorithms. From Table IV, the proposed algorithm exhibits significantly good recognition performance compared with the state-of-the-art conventional finger knuckle recognition algorithms.

F. Multibiometric Recognition

If there is a good general-purpose matching algorithm for biometric recognition, this matching algorithm is suitable to develop a compact and low-cost multibiometric system, since the system with multiple matching algorithms may become large and complex. Local phase features described in Sect. II-E can be used as general-purpose features for biometric recognition. Though a set of experiments for face, palmprint and finger knuckle recognition, we have demonstrated that local phase features exhibit efficient performance comparable with the state-of-the-art conventional algorithms [8]. The results indicate that the compact multibiometric systems can be developed using local phase features, since only one matching engine is required for calculating the matching scores for each biometric traits. Also, the matching scores are easily combined, since the matching scores are calculated based on the same criterion. In future, we will apply the local phase features to multibiometric systems and demonstrate the effectiveness of local phase features in multibiometric recognition problems.

IV. CONCLUSION

In this paper, we have introduced the novel biometric recognition algorithms using phase-based image matching. Our approach is primarily based on signal processing techniques, and hence is different from the conventional approaches which are based on computer vision, pattern recognition and image processing techniques. From a set of experiments, the use of phase information makes it possible to develop accurate biometric recognition algorithms. In other words, the signal processing technique is useful for biometric recognition problems. In future, we will explore the new biometric trait to develop a compact, easy-to-use and accurate person authentication system.

REFERENCES

- [1] CASIA iris image database. <http://www.idealtest.org/findTotalDbByMode.do?mode=Iris>.
- [2] FVC 2002. <http://bias.csr.unibo.it/fvc2002/>.
- [3] ICE 2005. <http://iris.nist.gov/ice/>.
- [4] PolyU FKP database. <http://www4.comp.polyu.edu.hk/~biometrics/FKP.htm>.
- [5] PolyU palmprint database. <http://www4.comp.polyu.edu.hk/~biometrics/>.
- [6] T. Ahonen, A. Hadid, and M. Pietikäinen. Face description with local binary patterns: Application to face recognition. *IEEE Trans. Pattern Anal. Mach. Intell.*, 28(12):2037–2041, Dec. 2006.
- [7] S. Aoyama, K. Ito, and T. Aoki. Finger-knuckle-print recognition using blpoc-based local block matching. *Proc. Asian Conf. Pattern Recognition*, pages 525–529, Nov. 2011.
- [8] S. Aoyama, K. Ito, and T. Aoki. Similarity measure using local phase features and its application to biometric recognition. *Proc. IEEE Computer Society Conf. Computer Vision and Pattern Recognition Workshop*, June 2013. (to be published).
- [9] J. Beveridge, D. Bolme, B. Draper, and M. Texeira. The CSU face identification evaluation system. *Machine Vision and Applications*, 16:128–138, 2005.
- [10] J. Daugman. High confidence visual recognition of persons by a test of statistical independence. *IEEE Trans. Pattern Anal. Mach. Intell.*, 15(11):1148–1161, Nov. 1993.
- [11] N. Duta, A. Jain, and K. Mardia. Matching of palmprints. *Pattern Recognition Letters*, 23(4):477–485, 2002.
- [12] P. H. Hennings-Yeomans, B. V. K. Vijaya Kumar, and M. Savvides. Palmprint classification using multiple advanced correlation filters and palm-specific segmentation. *IEEE Trans. Information Forensics and Security*, 2(3):613–622, Sept. 2007.
- [13] K. Ito, T. Aoki, T. Hosoi, and K. Kobayashi. Face recognition using phase-based correspondence matching. *Proc. IEEE Conf. Automatic Face and Gesture Recognition*, pages 173–178, Mar. 2011.
- [14] K. Ito, T. Aoki, H. Nakajima, K. Kobayashi, and T. Higuchi. A palmprint recognition algorithm using phase-only correlation. *IEICE Trans. Fundamentals*, E91-A(4):1023–1030, Apr. 2008.
- [15] K. Ito, S. Itsuka, and T. Aoki. A palmprint recognition algorithm using phase-based correspondence matching. *Proc. Int'l Conf. Image Processing*, pages 1977–1980, Nov. 2009.
- [16] K. Ito, A. Morita, T. Aoki, T. Higuchi, H. Nakajima, and K. Kobayashi. A fingerprint recognition algorithm combining phase-based image matching and feature-based matching. *Lecture Notes in Computer Science (ICB2006)*, 3832:316–325, Dec. 2005.
- [17] K. Ito, A. Morita, T. Aoki, H. Nakajima, K. Kobayashi, and T. Higuchi. Score-level fusion of phase-based and feature-based fingerprint matching algorithms. *IEICE Trans. Fundamentals*, E93-A(3):607–616, Mar. 2010.
- [18] K. Ito, H. Nakajima, K. Kobayashi, T. Aoki, and T. Higuchi. A fingerprint matching algorithm using phase-only correlation. *IEICE Trans. Fundamentals*, E87-A(3):682–691, Mar. 2004.
- [19] A. Jain, P. Flynn, and A. Ross. *Handbook of Biometrics*. Springer, 2008.
- [20] A. K. Jain, L. Hong, S. Pankanti, and R. Bolle. An identity-authentication system using fingerprints. *Proc. IEEE*, 85(9):1365–1388, Sept. 1997.
- [21] X. Jiang and W. Y. Yau. Fingerprint minutiae matching based on the local and global structures. *Proc. Int'l Conf. Pattern Recognition*, 2:1038–1041, Sept. 2000.
- [22] A. Kong, D. Zhang, and M. Kamel. Palmprint identification using feature-level fusion. *Pattern Recognition*, 39(3):478–487, Mar. 2006.
- [23] A. Kong, D. Zhang, and M. Kamel. A survey of palmprint recognition. *Pattern Recognition*, 42(7):1408–1418, Jan. 2009.
- [24] C. D. Kuglin and D. C. Hines. The phase correlation image alignment method. *Proc. Int'l Conf. Cybernetics and Society*, pages 163–165, 1975.
- [25] D. Maltoni, D. Maio, A. K. Jain, and S. Prabhakar. *Handbook of Fingerprint Recognition*. Springer, 2003.
- [26] L. Masek and P. Kovesi. MATLAB source code for a biometric identification system based on iris patterns. *School of Computer Science and Software Eng., Univ. Western Australia*, 2003.
- [27] K. Miyazawa, K. Ito, T. Aoki, K. Kobayashi, and H. Nakajima. An effective approach for iris recognition using phase-based image matching. *IEEE Trans. Pattern Anal. Mach. Intell.*, 30(10):1741–1756, Oct. 2008.
- [28] B. Moghaddam, C. Bastar, and A. Pentland. A bayesian similarity measure for direct image matching. *Proc. Int'l Conf. Pattern Recognition*, 2:350–358, 1996.
- [29] A. Morales, C. Travieso, M. Ferrer, and J. Alonso. Improved finger-knuckle-print authentication based on orientation enhancement. *IEEE Electronics Letters*, 47(6):380–381, Mar. 2011.
- [30] A. Oppenheim, R. Schafer, and J. Buck. *Discrete-Time Signal Processing (2nd Edition)*. Prentice Hall, 1999.
- [31] A. V. Oppenheim. The importance of phase in signals. *Proc. IEEE*, 69(5):529–541, May 1981.
- [32] P. Phillips, H. Moon, S. Rizvi, and P. Rauss. The FERET evaluation methodology for face recognition algorithms. *IEEE Trans. Pattern Analysis Machine Intelligence*, 22(10):1090–1104, Oct. 2000.
- [33] A. A. Ross, K. Nandakumar, and A. K. Jain. *Handbook of Multibiometrics*. Springer, 2006.
- [34] M. Savvides, B. V. K. V. Kumar, and P. K. Khosla. Eigenphases vs eigenfaces. *Proc. 17th Int'l Conf. Pattern Recognition*, 3:810–813, Aug. 2004.
- [35] K. Takita, T. Aoki, Y. Sasaki, T. Higuchi, and K. Kobayashi. High-accuracy subpixel image registration based on phase-only correlation. *IEICE Trans. Fundamentals*, E86-A(8):1925–1934, Aug. 2003.
- [36] K. Takita, M. A. Muquit, T. Aoki, and T. Higuchi. A sub-pixel correspondence search technique for computer vision applications. *IEICE Trans. Fundamentals*, E87-A(8):1913–1923, Aug. 2004.
- [37] M. Turk and A. Pentland. Eigenfaces for recognition. *J. Cognitive Neurosci.*, 3(1):71–86, 1991.
- [38] K. Venkataramani and B. V. K. Vijayakumar. Fingerprint verification using correlation filters. *Lecture Notes in Computer Science (AVBPA2003)*, 2688:886–894, June 2003.
- [39] L. Wiskott, J.-M. Fellous, N. Krüger, and C. von der Malsburg. Face recognition by elastic bunch graph matching. *IEEE Trans. Pattern Anal. Mach. Intell.*, 19(7):775–779, July 1997.
- [40] D. Zhang. *Palmprint Authentication*. Kluwer Academic Publication, 2004.
- [41] D. Zhang, W. Kong, J. You, and M. Wong. Online palmprint identification. *IEEE Trans. Pattern Anal. Mach. Intell.*, 25(9):1041–1050, Sept. 2003.
- [42] L. Zhang, L. Zhang, and D. Zhang. Finger-knuckle-print: A new biometric identifier. *Proc. Int'l Conf. Image Processing*, pages 1981–1984, Nov. 2009.
- [43] L. Zhang, L. Zhang, and D. Zhang. Finger-knuckle-print verification based on band-limited phase-only correlation. *Lecture Notes in Computer Science (CAIP2009)*, 5702:141–148, Sept. 2009.
- [44] L. Zhang, L. Zhang, D. Zhang, and Z. Guo. Phase congruency induced local features for finger-knuckle-print recognition. *Pattern Recognition*, 45:2522–2531, July 2012.
- [45] L. Zhang, L. Zhang, D. Zhang, and H. Zhu. Online finger-knuckle-print verification for personal authentication. *Pattern Recognition*, 43:2560–2571, July 2010.
- [46] L. Zhang, L. Zhang, D. Zhang, and H. Zhu. Ensemble of local and global information for finger-knuckle-print recognition. *Pattern Recognition*, 44:1990–1998, Sept. 2011.
- [47] W. Zhao, R. Chellappa, and A. Krishnaswamy. Discriminant analysis of principal components for face recognition. In Wechsler, Bruce, Fogelman-Soulie, and Huang, ed., *Face Recognition: From Theory to Applications*, pages 73–85, 1998.